Journal of Engineering and Sustainable Development
https://jeasd.uomustansiriyah.edu.iq/index.php/jeasd
https://doi.org/10.31272/jeasd.28.3.2

Vol. 28, No. 03, May 2024
ISSN 2520-0917

Original Research

PHASE ANGLE SHIFT AND SLOPE BASED RESTRAINT FOR INDIRECT SYMMETRICAL PHASE SHIFT TRANSFORMER PROTECTION

Shailendra Kumar Bhasker[1*], Manoj Tripathy[2]

[1]*Department of Electrical Engineering, Harcourt Butler Technical University, Kanpur, India*
[2]*Department of Electrical Engineering, Indian Institute of Technology, Roorkee, India*
[1] https://orcid.org/0009-0003-6473-031X
[2]https://orcid.org/0000-0001-8292-8870

Received 26/11/2023 ***Revised 16/03/2024*** ***Accepted 31/03/2024***

Abstract: This study presents a method to limit the functioning of the differential relay during the different operating conditions of an Indirect Symmetrical Phase Shift Transformer (ISPST). The proposed method depends on two thresholds; phase angle shift (PAS) between two ends of an ISPST to discriminate internal faults and inrush conditions from normal, over-excitation, and external fault conditions and slope of differential current helps to discriminate the situation of internal fault from inrush. In the first step of the algorithm, the PAS-based threshold discriminates normal, over-excitation, and external fault conditions from magnetizing inrush and internal fault conditions. In the second step, the slope-based threshold discriminates magnetizing inrush from internal fault conditions. The reliability of the proposed method has also been examined under the condition of current transformer saturation due to heavy external faults. Additionally, the comparison of the suggested and conventional methods is discussed to check the superiority of the proposed method. The proposed method eliminates the need for phase angle shift correction in the suggested method. A variety of faults in the series and excitation unit are simulated using the PSCAD/EMTDC platform to verify the approach method.

Keywords: *Differential protection; Inrush Current; Phase shift transformer; Power system relaying*

1. Introduction

Power flow over a particular line of a typical power transmission network is controlled by the Phase Shift Transformer (PST). Depending upon design, there are two types of PSTs: direct (single-core) and indirect (double-core). Direct PSTs are based on one 3-phase core. The phase shift is obtained by appropriately connecting the windings. Indirect PSTs are based on a construction with two separate transformers: one variable tap exciter to regulate the amplitude of the quadrature voltage and one series transformer to inject the quadrature voltage in the right phase. As a result, it may be classed as either symmetrical or asymmetrical [1] depending on the application. Symmetrical design PSTs modify the phase angle shift (PAS) only while the magnitudes of both ends voltages are identical, but asymmetrical design PSTs produce changes in PAS along with changes in the magnitude of both ends voltages which may cause a change in reactive power flow [2]. As opposed to asymmetrical PSTs, only the PAS affects the power flow in symmetrical PSTs [3]. The qualities and ease of construction of the Indirect Symmetrical PST (ISPST) depicted in Fig. 1 make it frequently utilized [4].

As a result of its significance, ISPST needs an advanced protection scheme for its security. ISPSTs are safeguarded using a variety of protection strategies including differential

**Corresponding Author*: skbhasker@hbtu.ac.in

protection, overload protection, over-excitation protection, backup protection, etc [5]. However, differential protection has served as a primary transformer safety strategy for decades. The protection of standard and non-standard phase shift transformers is traditionally provided by current differential protection [6, 7]. Furthermore, the common differential current measurement technique cannot be used for different PSTs because of the variety of PST designs and its non-standard phase shift. Several approaches based on differential current have been suggested for a variety of PSTs [8-10]. Differential protection of ISPST and Delta-hexagonal PSTs is discussed in [8, 9]. However, this technique needs 18 CTs, which makes differential protection quite costly. Top it all, these CTs are required to keep inside the PST. A method of phase angle shift compensation has been discussed for non-standard phase angle shifts between two ends to measure the differential current [10-11]. A delay in relay tripping is caused by the time it takes to do the computation for PAS compensation. It is, nevertheless, possible for differential protection to malfunction owing to un-faulted situations such as inrush, external fault due to non-standard phase angle shift, and current transformer (CT) saturation, which may lead to power system instability. To prevent differential protection from malfunctioning during magnetizing inrush, the harmonic restraint (HR) based approach is extensively utilized. Differential current, which is an important input to HR, has a second harmonic component that is much larger in inrush compared to internal fault current [5, 8]. As a result of their newer construction and material, contemporary transformers are more efficient and produce lower second harmonics inrush current, which has an impact on the HR scheme [2, 12]. The security of differential protection against CT saturation during external failures is another problem linked with its deployment. A differential current is increased in this situation, which may result in the differential relay malfunctioning [13, 14].

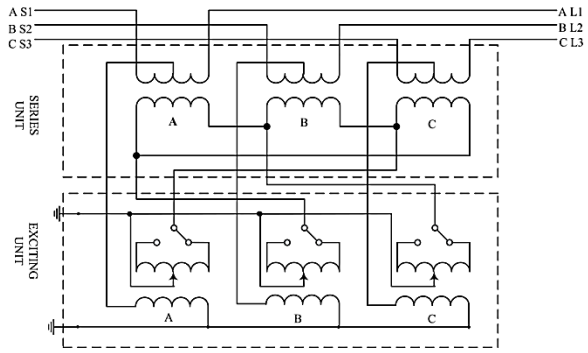

Figure 1. Line diagram of an ISPST [4]

Differential protection has been the focus of several recent solutions aiming at resolving the aforementioned issues. Artificial neural networks (ANN) [15- 18], fuzzy logic [19- 20], and wavelet analysis [21- 23] are some of the approaches that may be used. As a result, a large number of training data is required, the computational load on the differential relay is quite high, and the performance is highly dependent on the transformer parameter or starting conditions [13].

PAS and slope of differential thresholds are used in this paper to present a simple decision-making approach. Internal fault and inrush conditions are distinguished from normal, over-excitation, and external fault conditions by a PAS-based threshold. The non-standard phase angle shift of an ISPST does not affect the PAS-based threshold. To distinguish between an internal fault and a magnetizing inrush, a threshold based on the slope of differential current is used. The effect of CT saturation during an external fault scenario is also described here to check the reliability of the proposed method. Slope-based thresholds are

compared to the HR method for classification accuracy. Time-domain simulations demonstrate that the suggested approach is successful for internal fault conditions and boosts the relay's security against external fault, magnetizing inrush, and CT saturation.

2. Proposed Algorithm

During ISPST operation, it encounters one of the following conditions:

- Normal Condition
- Over-excitation Condition
- Magnetizing Inrush /Sympathetic Inrush Condition
- External Fault Condition
- Internal Fault Condition

In the absence of appropriate operating circumstances, the differential relay must operate only in the event of an internal fault. However, since the phase shift between the two ends of ISPST is non-standard, it is impacted by all operating conditions. The proposed approach is based on the PAS threshold between two ends of each phase, which is used to distinguish normal, over-excitation, and external fault conditions from inrush and internal fault conditions. Fig. 2 illustrates the normal operating state in advance and retard modes of operation with the maximum PAS and PAS threshold. Variation of phase angle shift will lie between the maximum value of PAS in both advance and retard mode of operation for any ISPST. An ISPST which has been considered for the illustration of the proposed method, has a maximum PAS of 30 degrees and -30 degrees in retard and advance mode of operation respectively. As seen in Fig. 3, the PAS-based threshold is unaffected by the condition of over-excitation. When magnetizing inrush occurs, PAS approaches 90 degrees due to its inductive behavior at no-load, as seen in Fig. 4. However, during on-load magnetization, PAS becomes less than 90 degrees due to the ISPST's retard mode of operation. When an internal fault occurs in any unit of ISPST, either the source-side current or the load-side current is reversed and the PAS between them exceeds 90 degrees, as seen in Fig. 5. However, in the event of an inter-turn fault, the PAS is not larger than 90 degrees because the current is not reversed on either the source or load side. Similarly, in the event of an external failure, there is no current reversal at any end of an ISPST, and so the PAS between two ends current tends to zero, as seen in Fig. 6. As a result, a PAS-based threshold may distinguish inrush and internal fault condition from other above-mentioned operating conditions.

A) Calculation of PAS threshold i.e. threshold1:

The PAS threshold is determined by considering magnetizing inrush in both no-load and loaded conditions. PAS is roughly equal to 90 degrees in the absence of load as discussed earlier but decreases to less than 90 degrees in the presence of load owing to the retard mode of an ISPST. As a result, the PAS threshold is computed by (1)

$$\text{PAS threshold (threshold1)} = (-90+\Delta\theta_{rmax}) \quad (1)$$

Where $\Delta\theta_{rmax}$ is the maximum PAS in retard mode of operation

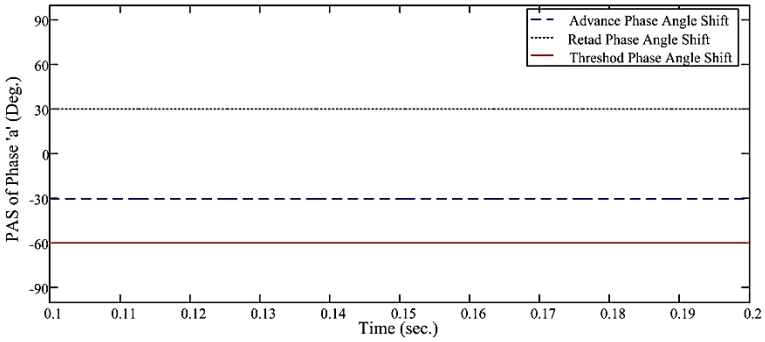

Figure 2. Phase 'a' PAS during normal operation of an ISPST

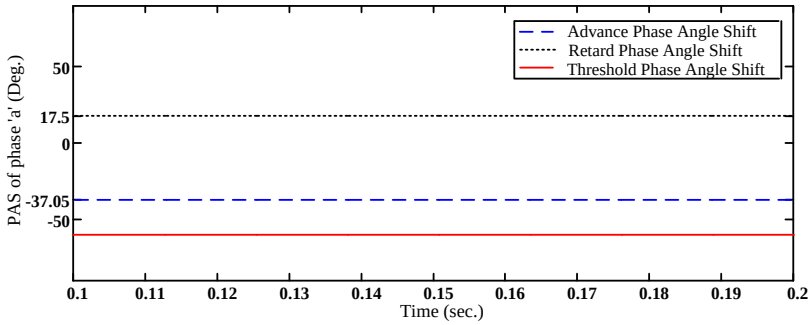

Figure 3. Phase 'a' PAS during over-excitation of an ISPST

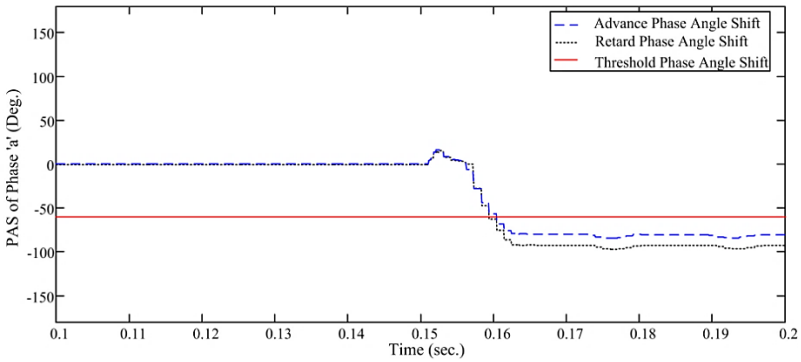

Figure 4. Phase 'a' PAS during energization of an ISPST at t=0.15sec. (zero degree)

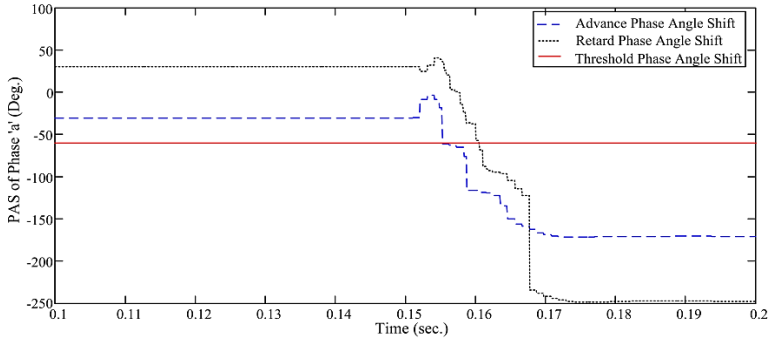

Figure 5. Phase 'a' PAS when an internal fault (A-G) occurred in the excitation unit of an ISPST at t=0.15sec.(zero degree)

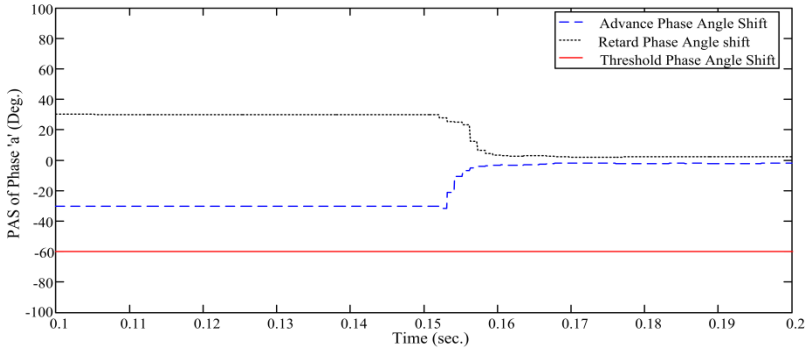

Figure 6. Phase 'a' PAS when an external fault (A-G) occurred at t=0.15sec. (zero degree)

After the identification of internal fault and inrush conditions, the next step is to discriminate the internal fault from inrush. To discriminate the faulty conditions from inrush, the following characteristic of the differential current is considered as shown in Fig. 7.

- When there is a magnetizing inrush condition, the waveform has a large slope near the peak.
- When there is an internal fault condition, the waveform has a low slope near the peak.

Using this feature, internal fault conditions can easily be distinguished from magnetizing inrush conditions.

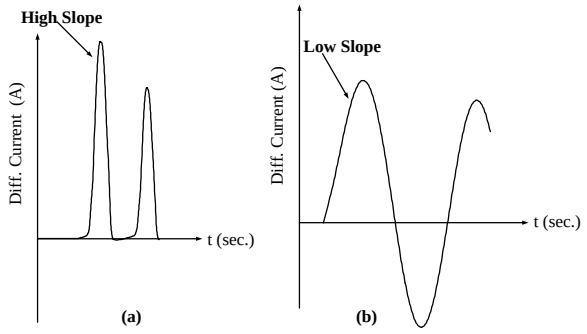

Figure 7. The behavior of differential current of ISPST under (a) Inrush and (b) Faulty condition [24]

B) Methodology to calculate slope:

Let us consider that, the first peak of differential current comes at the k^{th} sample after the identification of inrush or faulty condition with the help of PAS threshold (threshold1). A window of the 'k' sample will be generated after threshold 1. This data window is normalized by the k^{th} (max value) sample to get slope according to per unit data window. Let's normalized data window is given by (2):

$$X = [x_1, x_2, \dots\dots\dots x_k] \quad (2)$$

The slope is calculated by (3)

$$Slope = \frac{(x_{k-c1} - x_{k-c2})}{(t_{k-c1} - t_{k-c2})} \quad \text{for } c2 > c1 \quad (3)$$

Where 't' is time; c1,c2 are constant depends on sampling frequency

After calculating the slope, a slope threshold i.e. threshold2 is decided by analyzing the maximum possible fault conditions. Fig. 8 shows the flow chart for the proposed method.

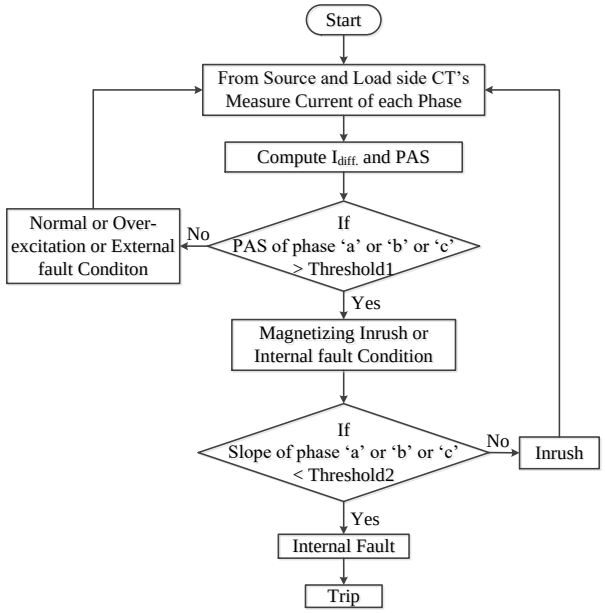

Figure 8. Flowchart of the proposed method

3. Simulation and Results

To demonstrate the effectiveness of the proposed method, 3-ϕ, 300MVA, 138kV/138kV, 1255A/1255A, 60Hz ISPST with max phase shift of ±30 degrees and maximum loading of 240MW and 180MVAR is simulated using PSCAD/EMTDC platform as shown in Fig. 9 [25]. At both ends of an ISPST, relevant CTs with a ratio of 2000/5A are connected in a star configuration.

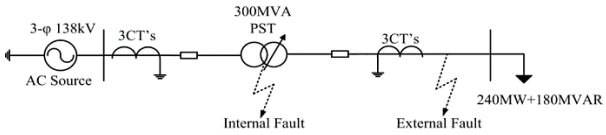

Figure 9. Schematic diagram of the simulated model

To simulate the inrush condition, the switching in angle, the loading condition, and the remanent flux in the core are taken into account. The PAS threshold is calculated by (1)

PAS threshold (threshold1) = (–90+Δθrmax)

For this paper, Δθrmax is 30 degrees hence PAS threshold is –60 degrees.

The slope of differential current signals is calculated by using (3) and summarized in Table 1.

Similarly, the slope of differential current for verities of internal fault is calculated by using (3) with different fault inception angles for both advance and retard phase angle shift at no-load and on-load conditions. Tables 2 and 3 summarize the slope of differential current for verities of internal fault in excitation and series units respectively. The slope of differential current for occurrence of inrush and internal fault simultaneously is also shown in Table 4.

From the tables, it is clear that the minimum slope of differential current is 104.81in the case of magnetizing inrush and the maximum slope of differential current is 102.25 for internal fault. Hence the threshold of slope is calculated by the mean of these two slopes which is given by (4).

$$Slope\ threshold = \frac{Min.slope\ of\ magnetizing\ inrush + Max.slope\ of\ Internal\ fault}{2} \quad (4)$$

Hence the slope threshold (threshold2) for this paper is 103.53.

Table 1: The slope of the differential current for each phase of the inrush current

% Residual flux	Switching Angle (Deg.)	Phase	Slope			
			Retard PAS		Advance PAS	
			On-Load	No-Load	On-Load	No-Load
0%	0	a	129.33	177.32	146.89	154.84
		b	271.09	147.56	123.60	127.59
		c	197.41	156.14	208.51	205.29
	60	a	345.19	262.20	121.12	126.82
		b	154.17	218.76	201.38	198.21
		c	143.49	124.39	141.67	149.60
	90	a	183.11	235.21	149.16	189.29
		b	196.64	195.21	198.88	173.77
		c	148.66	162.95	178.76	185.35
50%	0	a	218.11	183.88	399.86	130.78
		b	133.85	247.30	222.59	129.11
		c	123.42	237.36	120.56	239.92
	60	a	147.66	147.66	473.60	148.69
		b	133.52	152.80	188.43	183.53
		c	175.51	133.87	189.21	236.94
80%	0	a	195.71	177.27	266.61	142.94
		b	167.70	317.07	156.85	148.88
		c	187.28	122.62	**104.81**	138.92
	60	a	157.63	159.55	353.00	176.79
		b	214.07	324.89	476.45	212.63
		c	157.63	208.43	105.05	144.71
	90	a	173.23	224.46	152.24	215.89
		b	332.48	159.63	178.26	136.94
		c	170.23	167.33	152.84	215.89

Table 2. The slope of each phase differential current for internal fault in the Excitation Unit

Inception angle of a fault (Deg.)	Type of Fault	Phase	Slope			
			Retard PAS		Advance PAS	
			On-Load	No-Load	On-Load	No-Load
0	Inter-turn in phase 'a'	a	73.15	74.25	68.04	78.20
		b	72.54	73.59	74.42	73.25
		c	71.65	72.67	71.20	79.30
	A-G	a	73.25	70.95	66.04	71.74
		b	73.64	73.84	74.20	70.62
		c	72.34	73.19	70.20	71.32
	A-B	a	88.90	87.89	89.12	100.23
		b	82.45	83.55	82.36	100.92
		c	70.93	68.36	85.78	88.09
	A-B-G	a	77.62	79.34	89.00	86.41
		b	80.28	82.28	101.09	101.14
		c	76.83	82.12	85.09	75.66
	A-B-C	a	77.76	88.30	71.18	71.43
		b	101.88	98.08	101.11	100.90
		c	99.29	99.52	97.66	94.40
	A-B-C-G	a	72.76	89.30	70.18	70.43
		b	100.88	98.08	100.11	99.93
		c	98.29	100.52	96.56	93.39

		a	87.74	94.02	88.25	88.72
	A-G	b	95.30	90.14	85.30	90.56
		c	87.64	94.62	86.57	87.72
		a	67.34	72.03	89.49	99.60
	A-B	b	74.88	99.50	100.17	100.61
		c	67.34	72.03	88.42	98.60
60		a	65.85	68.69	84.06	83.45
	A-B-G	b	99.53	101.21	101.27	100.05
		c	65.85	67.69	83.42	82.50
		a	97.08	100.85	99.70	98.14
	A-B-C	b	100.74	101.06	86.25	101.84
		c	97.68	99.96	98.60	97.67
		a	97.08	100.85	101.70	99.14
	A-B-C-G	b	101.74	101.24	**102.25**	100.84
		c	97.88	99.99	96.70	99.67
		a	88.71	93.81	90.06	91.41
	A-G	b	96.08	91.77	86.37	90.35
		c	87.75	92.80	91.83	91.78
		a	68.34	70.65	77.85	77.90
90	A-B-G	b	100.30	92.68	100.66	100.74
		c	69.84	72.66	77.05	77.96
		a	99.19	100.85	87.49	100.74
	A-B-C-G	b	100.00	99.00	96.27	96.47
		c	99.49	100.99	89.48	99.74

Table 3. The slope of each phase differential current for internal fault in Series Unit

Inception angle of a fault (Deg.)	**Type of Fault**	**Phase**	**Slope**			
			Retard PAS		**Advance PAS**	
			On-Load	**No-Load**	**On-Load**	**No-Load**
		a	83.08	94.00	87.01	95.00
	Inter-turn	b	95.60	94.002	90.48	95.06
	in phase ‘a’	c	82.07	94.79	86.38	94.89
		a	83.64	97.63	85.69	88.72
	A-G	b	92.94	98.20	93.32	93.81
		c	83.99	97.78	99.21	89.73
0		a	62.52	67.83	73.07	67.37
	A-B	b	99.52	94.71	77.32	82.97
		c	99.31	98.80	80.82	85.16
		a	83.44	94.08	100.38	85.98
	A-B-G	b	100.10	99.65	91.13	97.96
		c	99.64	90.04	97.46	92.69
		a	78.89	76.42	85.64	78.75
	A-B-C-G	b	100.57	100.40	93.51	92.06
		c	99.82	98.72	100.20	100.82
		a	97.30	84.44	94.20	93.29
	A-G	b	94.53	92.71	90.68	95.00
		c	85.34	97.48	97.82	93.40
		a	63.86	71.88	85.30	78.97
60	A-B	b	78.18	83.50	62.64	57.73
		c	95.60	98.79	97.05	96.85
		a	95.36	100.75	96.68	79.66
	A-B-G	b	83.01	84.43	73.84	66.41
		c	100.07	99.95	85.78	63.19

		a	84.59	85.36	95.43	88.47
	A-B-C-G	b	69.23	74.59	65.64	72.20
		c	68.49	69.39	75.83	68.43
		a	89.78	88.97	91.38	89.63
	A-G	b	91.93	90.01	87.81	92.97
		c	89.07	94.33	95.32	89.07
		a	97.51	96.97	95.73	96.98
90	A-B-G	b	93.32	92.84	92.91	92.21
		c	100.40	93.63	91.59	87.20
		a	98.17	99.54	89.39	95.25
	A-B-C-G	b	90.29	87.01	83.43	88.11
		c	101.94	100.76	100.11	99.64

Table 4. The slope of differential current for the occurrence of inrush and internal fault simultaneously

Switching Angle (Deg.)	Phase	Slope	
		Retard Phase Shift	Advance Phase Shift
	A	87.78	87.58
0	B	70.47	95.67
	C	95.75	87.51
	A	87.75	89.29
60	B	91.21	90.29
	C	98.27	89.36
	A	89.25	91.63
90	B	92.54	95.08
	C	97.81	91.76

Out of these cases, few typical cases are discussed in the paper due to the limitation of pages. Fig. 10 shows the proposed relay operation for magnetizing inrush. Fig. 10(a) shows the phase 'a' differential current and Fig. 10(b) shows phase 'a' PAS between two ends of an ISPST. When the PAS of phase 'a' is less than the threshold1 value, the trip signal will become high to calculate the slope of differential current as shown in Fig. 10(c). If the slope is greater than the threshold value (threshold2), the final trip signal will not be high as shown in Fig. 10(d).

Fig. 11 shows the proposed relay operation to the A-G internal fault in the excitation unit for advanced PAS of an ISPST. Fig. 11(a) shows the phase 'a' differential current and Fig. 11(b) shows the PAS of phase 'a' between two ends of an ISPST. When the PAS of phase 'a' lies down the threshold1 as shown in Fig. 11(c), the PAS trip signal will be high to calculate the slope of differential current. If the slope is less than the threshold value (threslod2), the final trip signal will be high as shown in Fig. 11(d). From Fig. 11(d) it is clear that the operating time of the relay is 6.0 msec. Similarly, Fig. 12 shows the proposed relay operation to an internal fault in a series unit and the operating time is 20.5msec. From Fig. 13, it is very clear that the operating quantity (PAS) lies above the threshold1 to external fault condition, and the PAS trip signal will not be high for the next step. Hence this method is unaffected by external fault without any phase shift compensation in both advance and retard PAS.

(a) Magnetizing Inrush Following Internal Fault

The performance of the proposed method is also examined for magnetizing inrush following internal fault conditions. An ISPST is switched on at 0.15 sec. and internal fault (A-G) also occurs at the same time in phase 'a' of the excitation unit with retard phase angle shift. From Fig. 14, it is clear that the final trip signal is high after 24msec. of internal fault.

(b) Effect of CT saturation caused by external fault

In order to study the performance of the proposed method due to CT saturation caused by AB-G external fault, the load-side CT of phase 'a' is forced to saturate by increasing the CT secondary burden up to 300 ohm. The flux density of the CT is shown in Fig. 15(a). The distorted phase ‘a’ current waveform is shown in Fig. 15(b). Fig. 15 (c) shows the PAS of phase 'a' with its threshold1 with retard phase angle shift and it is clear that the operating quantity (PAS) lies above the threshold1 due to CT saturation and no trip signal is high for the next step as shown in Fig. 15 (d).

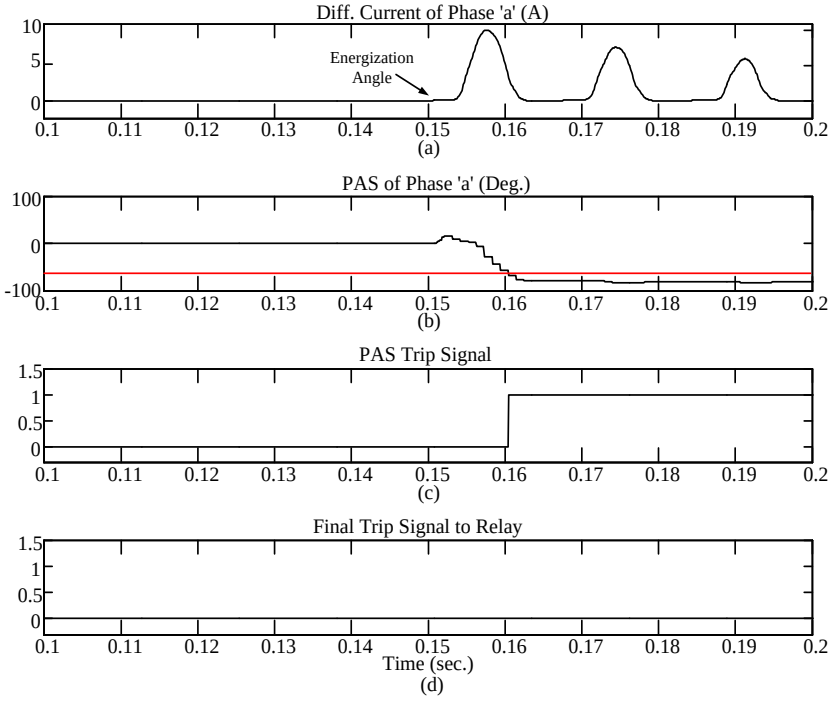

Figure 10. Response of proposed method to the magnetizing inrush; (a) phase 'a' differential current, (b) PAS of phase 'a' and threshold2, (c) PAS trip signal, and (d) final trip signal

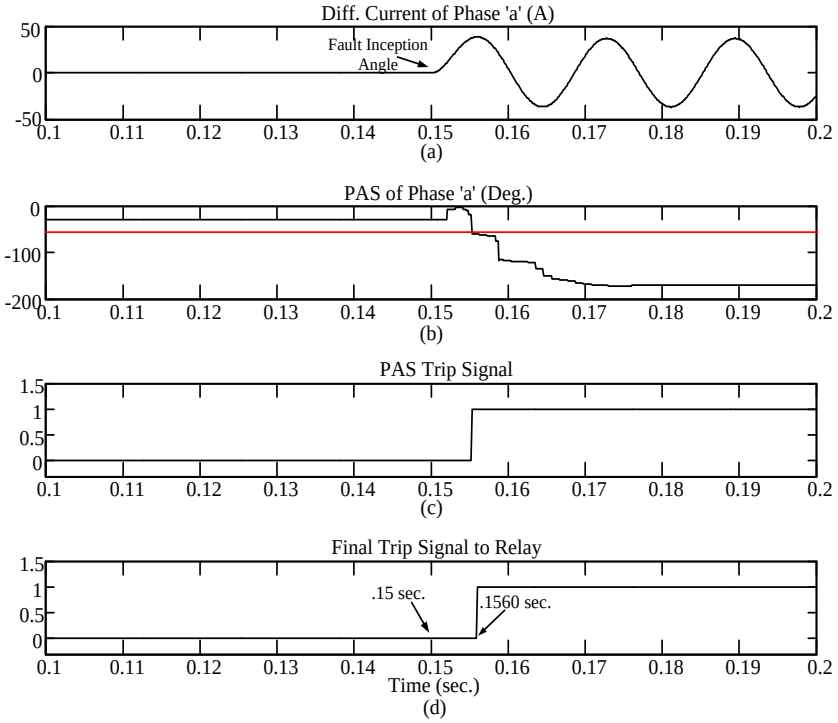

Figure 11. Response of proposed method to an internal fault (A-G) in excitation unit; (a) phase 'a' differential current, (b) PAS of phase 'a' and threshold2, (c) PAS trip signal and (d) final trip signal

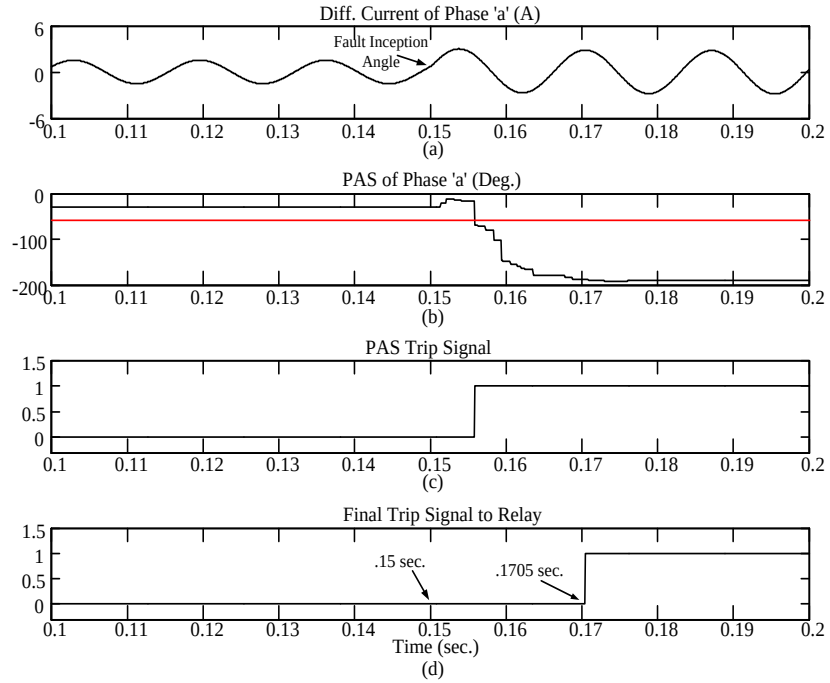

Figure 12. Response of proposed method to an internal fault (A-G) in the series unit; (a) phase 'a' differential current, (b) PAS of phase 'a' and threshold2, (c) PAS trip signal, and (d) final trip signal

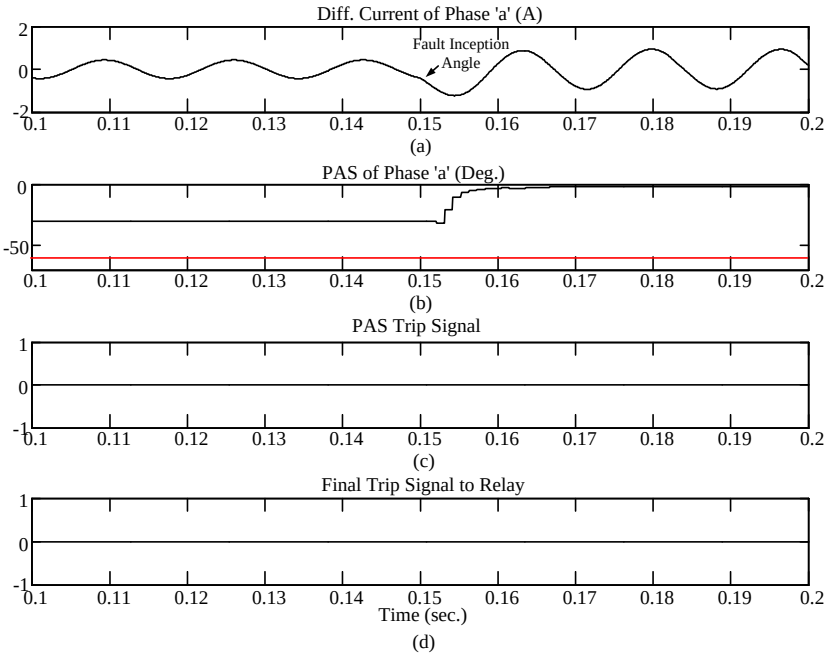

Figure13.Response of proposed method to an external fault (A-G); (a) phase 'a' differential current, (b) PAS of phase 'a' and threshold2, (c) PAS trip signal, and (d) final trip signal

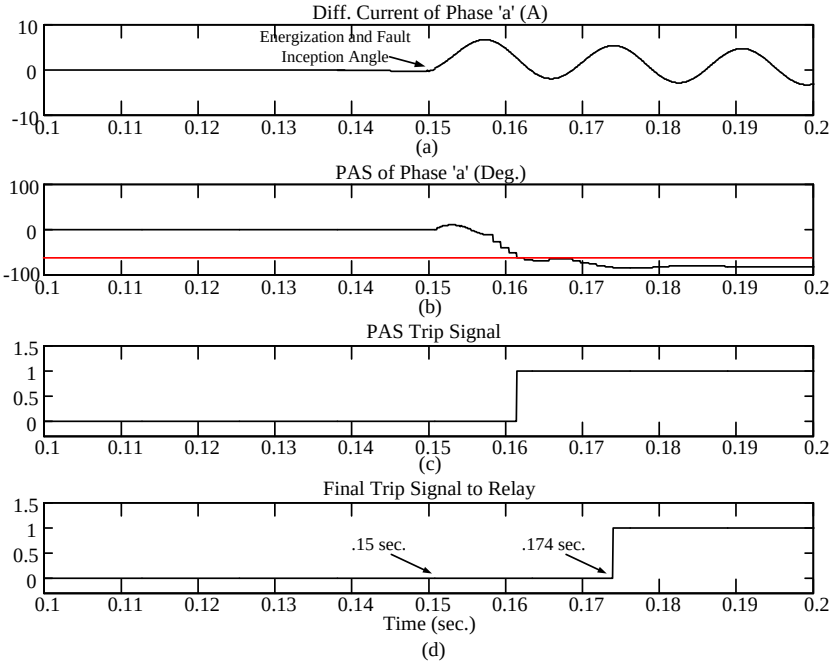

Figure 14. Response of proposed method to simultaneous inrush and internal fault; (a) phase 'a' differential current, (b) PAS of phase 'a' and threshold2, (c) PAS trip signal, and (d) final trip signal

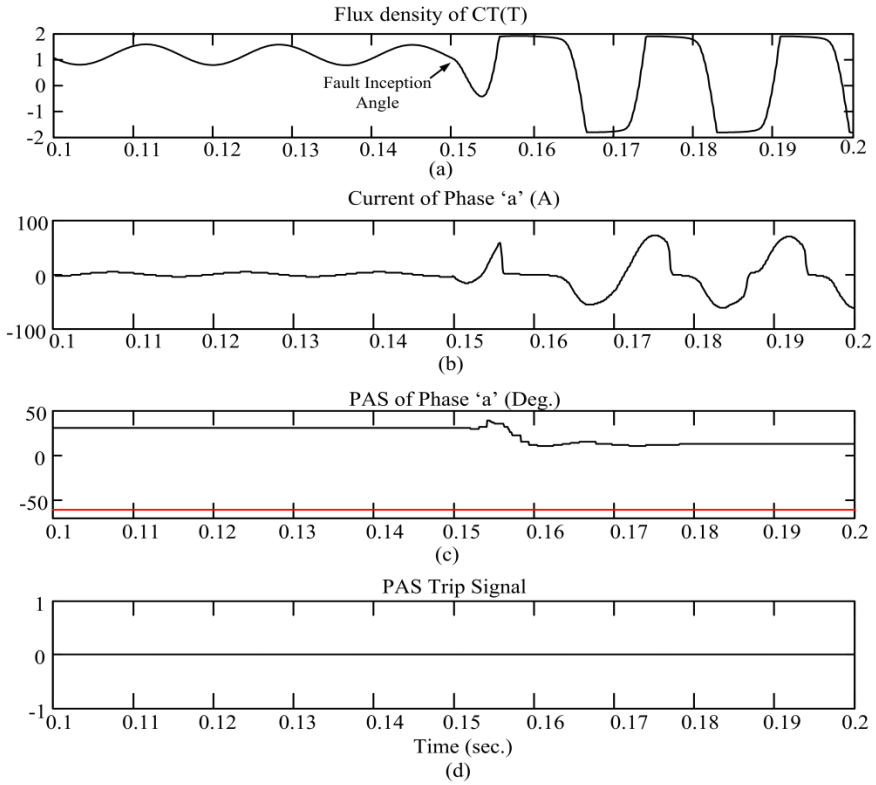

Figure 15. Response of proposed method for CT saturation during external fault; (a) Flux density (b)load-side phase 'a' current, (c) PAS of phase 'a' and threshold2, (d) PAS trip signal

4. Comparison of Proposed and Conventional Approaches

This study compares the performance of our new proposed method to discriminate between internal fault and other conditions with FFT-based HR considering PAS compensation. The ratio of the second harmonic to fundamental of the differential current for typical internal failure and inrush conditions are shown in Fig. 16(a and b) respectively. From Fig. 16, it appears that in an internal failure situation, the ratio of second harmonic to fundamental is greater than a condition of magnetizing inrush. Due to this condition, a conventional relay with HR will malfunction. Whereas the proposed method based on slope characteristics discriminates these two conditions. As a result, it is immune to the different harmonics in operating signals, making it more simple and robust than conventional relays.

The performance of the proposed approach for various internal faults in series and excitation units during the advance and retard PAS is summarized in Tables 5 and 6. Table 7 shows the operating time for the occurrence of internal fault and inrush simultaneously. The percentage of faulty winding is taken from a neutral point.

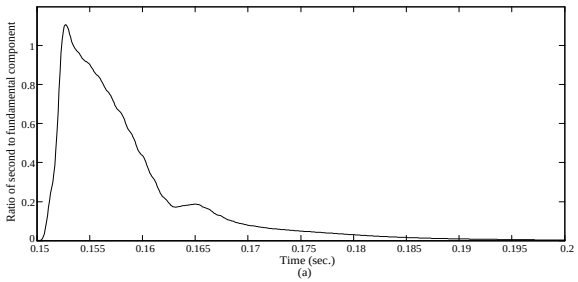

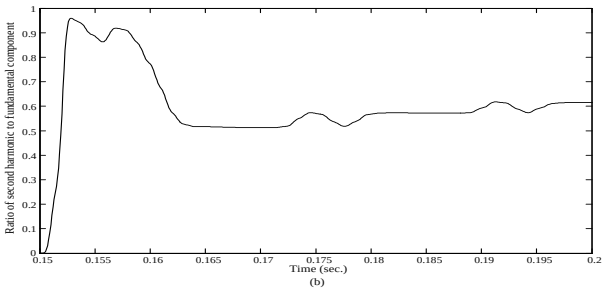

Figure 16. The ratio of the second harmonic to fundamental of the differential current for (a) internal fault condition and (b) inrush condition

Table 5: Operating time of proposed relay for internal fault in excitation unit

Fault Type	Operating Time (msec.)	
	Proposed Relay	Conventional approach
A-G (5%)*	6.0	20.5
A-G (10%) **	2.8	22.4
A-G (20%)*	23.3	30.2
A-G (40%) **	23.7	29.3
A-G (60%)*	23.6	29.3
A-B*	23.3	30.5
A-B**	6.6	25.6
A-B-G*	5.1	22.4
A-B-G**	5.3	22.4
A-B-C-G*	23.5	30.3
A-B-C-G**	23.3	30.2

*For Advance PAS
**For Retard PAS

Table 6: Operating time of proposed relay for internal fault in series unit

Fault Type	Operating Time (msec.)	
	Proposed Relay	Conventional approach
T-T (5%)*	20.5	Fail
T-T (10%) **	26.9	Fail
T-T (20%)*	27.0	Fail
A-G (10%) **	19.7	29.2
A-G (20%)*	19.7	30.0
A-G (50%)*	19.7	29.9
A-B*	7.8	27.8
A-B**	22.1	26.3
A-B-G*	20.3	26.3
A-B-G**	19.6	26.3
A-B-C-G*	24.4	30.3
A-B-C-G**	24.5	30.3

*For Advance PAS
** For Retard PAS

Table 7: Operating Time of Proposed relay for occurrence of internal fault and inrush simultaneously

Fault Type	Operating Time (msec.)	
	Proposed Relay	Conventional approach
Inrush & A-G (5%)	26.0	27.1
Inrush & A-G (20%)	24.0	27.1
Inrush & A-B*	19.2	28.8
Inrush & A-B**	6.4	30.2
Inrush & A-B-G*	23.0	27.5
Inrush & A-B-G**	6.6	27.5
Inrush & A-B-C-G*	24.4	31.2
Inrush & A-B-C-G**	24.5	31.1

*For Advance PAS
** For Retard PAS

5. Conclusion

A new algorithm for the protection of an ISPST based on two thresholds is proposed in this paper. The PAS threshold (threshold1) is utilized to discriminate magnetizing inrush and internal fault conditions from other operating conditions. Whereas slope-based threshold (threshold2) is considered for the discrimination of inrush condition from internal fault condition. The suggested method also detects internal faults following magnetizing inrush. Additionally, the reliability of the proposed method is also proved by considering CT saturation caused by an external fault.

The simulations demonstrate that the proposed algorithm is capable of improving the performance of differential relays for the protection of ISPST. The obtained findings demonstrate that the proposed algorithm is accurate and that it is also capable of stabilizing the differential relay in its non-faulty conditions. The advantage of the algorithm is that it does not require compensation of phase angle shift in either the advance or retard mode of an ISPST which reduces the time and cost of the protection.

Conflict of interest

The authors declare that there are no conflicts of interest regarding the publication of this manuscript.

Author Contribution Statement

The author, Shailendra Kumar Bhasker, presented the research problem and analyzed the theory according to analytical methods. The author, Manoj Tripathy, supervised and verified the final analysis results of the research.

References

1. J. Verboomen, D. Van Hertem, P. Schavemaker, W. Kling, and R. Belmans, “Phase Shifting Transformers: Principles and Applications,” IEEE Conference on Digital Object Identifier, pp. 1-6, 18 Nov 2005. https://doi.org/10.1109/FPS.2005.204302.
2. U. N. Khan, T. S. Sidhu, "Protection of standard-delta phase shift transformer using terminal currents and voltages," Electric power systems research, vol. 110, pp. 31-38, May 2014. https://doi.org/10.1016/j.epsr.2013.12.017
3. H. H. James, Electric Power Transformer Engineering, CRC Press LLC, Boca Raton, FL, 2004, pp. 84–102. https://doi.org/10.1201/b12110.
4. M. A. Ibrahim and F. P. Stacom, “Phase angle regulating transformer protection,” IEEE Trans. Power Del., vol. 9, no.1, pp.394 – 404, Jan. 1994. https://doi.org/10.1109/61.277711.
5. J. Blade and A. Montoya, “Experiences with parallel EHV phase shifting transformers,” IEEE Trans. Power Del., vol. 6, no. 3, pp. 1096–1100, July 1991. https://doi.org/10.1109/61.85853.
6. IEEE Guide for Protecting Power Transformers," in IEEE Std C37.91-2021 (Revision of IEEE Std C37.91-2008), vol., no., pp.1-160, 29 June 2021, https://doi.org/10.1109/IEEESTD.2021.9471045.
7. P. Ni, J. Zhang, J. Liang, X. Li, and Z. Liu, "A Study of the Effect of Phase Shifting Transformers on Line Longitudinal Differential Protection," 2023 3rd International Conference on Energy, Power and Electrical Engineering (EPEE), Wuhan, China, 2023, pp. 654-660, https://doi.org/10.1109/EPEE59859.2023.10351817.
8. IEEE Power System Relaying Committee: Working Group K1, “Protection of Phase Angle Regulating Transformers,” IEEE Power System Relaying Committee: Working Group K1, 1999.
9. Hossam A. Abd el-Ghany, Ismail A. Soliman, Ahmed M. Azmy, “A reliable differential protection algorithm for delta hexagonal phase-shifting transformers”, International Journal of Electrical Power & Energy Systems, vol. 127, 2021, 106671. https://doi.org/10.1016/j.ijepes.2020.106671
10. Z. Gajic, “Use of Standard 87T Differential protection for special three-phase power transformers-Part I: Theory,” IEEE Transaction on Power Delivery, vol. 27, no. 3, pp 1035-1040, July 2012.

https://doi.org/10.1109/TPWRD.2012.2188650.

11. T. Hayder, U. Schaerli, K. Feser, L. Schiel, "Universal adaptive differential protection for regulating transformers" IEEE Transactions on Power Delivery, vol. 23, no. 2, pp. 568-575, April 2008. https://doi.org/10.1109/TPWRD.2008.916758.
12. C. Mo, T.Y. Ji, L.L. Zhang, Q.H. Wu, "Equivalent statistics based inrush identification method for differential protection of power transformer", Electric Power Systems Research, Vol. 203, 2022. https://doi.org/10.1016/j.epsr.2021.107664
13. H. Dashti and M. Sanaye-Pasand, "Power Transformer Protection Using a Multiregion Adaptive Differential Relay" IEEE Transaction on Power Delivery, vol. 29, no. 2, pp 777-785, April 2014. https://doi.org/10.1109/TPWRD.2013.2280023.
14. Seyed Masood Lal Moosavi, Yaser Damchi, Mohsen Assili, "A new fast method for improvement of power transformer differential protection based on discrete energy separation algorithm", International Journal of Electrical Power & Energy Systems, Vol. 136, 2022, https://doi.org/10.1016/j.ijepes.2021.107759
15. A. H. Shah, A. H. Miry, T. M. Salman "Automatic Modulation Classification Using Deep Learning Polar Feature", *J. eng. sustain. dev.*, vol. 27, no. 4, pp. 477–486, Jul. 2023, https://doi.org/10.31272/jeasd.27.4.5.
16. M. Tripathy, R. P. Maheshwari, and H. K. Verma, "Power Transformer Differential Protection Based On Optimal Probabilistic Neural Network," IEEE Transactions on Power Delivery, vol. 25, no. 1, pp. 102-112 January 2010. https://doi.org/10.1109/TPWRD.2009.2028800.
17. A. N. Hamoodi, M. A. Ibrahim, B. M. Salih, "An intelligent differential protection of power transformer based on artificial neural network," Bulletin of Electrical Engineering and Informatics, vol. 11, no. 1, pp. 93-102, February 2022. https://doi.org/10.11591/eei.v11i1.3547
18. S. Afrasiabi, M. Afrasiabi, B. Parang, and M. Mohammadi, "Designing a composite deep learning based differential protection scheme of power transformers," Applied Soft Computing, vol. 87, February 2020. https://doi.org/10.1016/j.asoc.2019.105975
19. M. A. Ali, A. H. Mir, T. M. Salman "Implementation Of Artificial Intelligence In Controlling The Temperature Of Industrial Panel", *J. eng. sustain. dev.*, vol. 25, no. 1, pp. 92–99, Jan. 2021, https://doi.org/10.31272/jeasd.25.1.8
20. V.K. Sahu and Y. Pahariya, "Transformer Protection Improvement Using Fuzzy Logic," Design Engineering, vol. 2021, no. 9, pp 4914 – 4926, 2021. https://doi.org/10.31838/ecb/2023.12.s3.008

21. A. Majeed Mohammed, “Investigation Image Compression Using Nondyadic Wavelet Transform and Fast Zero Tree Algorithm”, J. eng. sustain. dev., vol. 15, no. 1, pp. 216–223, Mar. 2011. https://jeasd.uomustansiriyah.edu.iq/index.php/jeasd/article/view/1362.

22. S. S. D. Sahel, M. Boudour “Wavelet energy moment and neural networks-based particle swarm optimisation for transmission line protection,” Bulletin of Electrical Engineering and Informatics, vol. 8, no. 1, pp. 10-20, March 2019. https://doi.org/10.11591/eei.v8i1.1214

23. R. P. Medeiros, F. Bezerra Costa, K. Melo Silva, J. d. J. C. Muro, J. R. L. Júnior and M. Popov, "A Clarke-Wavelet-Based Time-Domain Power Transformer Differential Protection," IEEE Transactions on Power Delivery, vol. 37, no. 1, pp. 317-328, Feb. 2022. https://doi.org/10.1109/TPWRD.2021.3059732

24. J. Faiz and S. Lotfi-Fard, "A novel wavelet-based algorithm for discrimination of internal faults from magnetizing inrush currents in power transformers," in IEEE Transactions on Power Delivery, vol. 21, no. 4, pp. 1989-1996, Oct. 2006, https://doi.org/10.1109/TPWRD.2006.877095

25. D. A. Tziouvaras, “Protecting a 138 KV Phase Shifting Transformer: EMTP Modeling and Model Power System Testing,” 46th Annual Georgia Technical Protective Relay Conference, pp. 1–15, 2002.